

Selection Of Wind Sail Profile Using Computational Fluid Dynamics

K Prasanth¹, Preetha Varghese², Balakrishnan C R³

¹*Principal, Holy Grace Academy of Engineering*

²*Professor, Sree Narayana Gurukulam College of Engineering*

³*Lecturer, Holy Grace Polytechnic College*

Abstract—The marine industry is highly dependent on oil as fuel and the increased consumption of this fast-depleting oil resource creates a shortage of fuel for the future as well as pollutes the environment and seriously affects marine life. Also, the oil price is very high these days. Thus, the need for an alternate sustainable fuel source is of great importance. One such feasible alternative energy source is wind energy. The abundance, free availability and ease of conversion makes it an ideal alternative to oil, this wind energy can be extracted by sails. This project involves analysis of different types of aero foil geometries (NACA0012, NACA0015, NACA0018, NACA0020) at 11 different wind angles and picking out the most efficient type. Then, the geometry of the selected airfoil is modified by bending the trailing edge at various positions of chord length and thereby selecting the most optimum design by considering the factors such as variation of forward thrust, lateral thrust, corresponding to different tip angles with the help of computational fluid dynamics at different wind angle. NACA 0018 is opted out among these four airfoils. The modified geometry of NACA0018 at 40% chord length by 30-degree flap angle is selected as the most optimum wind sail profile.

Index Terms—Aerofoil geometries, NACA(National Advisory Committee for Aeronautics) aerofoils, Computational Fluid Dynamics.

I. INTRODUCTION

Fossil fuels power global maritime transport, consuming 1680 million barrels of petroleum annually, costing \$132 billion, and accounting for 12% of global petroleum use. With 90% of global trade relying on shipping, rising fuel costs and emissions pose economic and environmental challenges. Ships primarily use heavy fuel oil, which has high sulfur content, releasing harmful sulfur oxides (SOx) and nitrogen oxides (NOx). Shipping

contributes 13% of human-caused SOx and 15% of NOx emissions, worsening air pollution and climate change.

Regulatory measures aim to curb emissions, yet projections suggest maritime transport emissions could rise by 50-250% by 2050. The industry is exploring alternative fuels and efficiency improvements, but progress remains slow. Wind-assisted propulsion saw a brief revival in the 1980s, yet sustainable solutions are still needed. Ship owners and marine engineers continue to seek cost-effective, eco-friendly alternatives to reduce dependence on fossil fuels while maintaining operational efficiency.

II. LITERATURE REVIEW

K. Prasanth [1] studied aerofoil NACA0018, optimizing tip modifications for maximum forward thrust and minimal lateral thrust. Viola I. M. et al. (2008) conducted CFD feasibility studies for yacht aerodynamics, confirming its reliability. Chapin V. G. et al. (2008) evaluated the ADONF software for optimizing complex sail designs using RANS simulations. Collie S. J. et al. (2002) performed parametric design analysis of downwind sails for ACC using CFD. Alza P. A. et al. (2010) validated 3D RANS simulations with full-scale racing boat data.

Pravesh Chandra S. et al. (2009) developed software to optimize wing-sail positioning, estimating 8.3% fuel savings. Siulisetyono A. et al. (2010) numerically analyzed sail forces with CFD, verifying results through wind tunnel tests. Riotte Met. et al. (2014) explored yacht trimming using RBF mesh morphing. Flay R. et al. (2011) compared full-scale, wind tunnel, and CFD results for sail performance analysis. Francisco Perez A. et al. (2012) studied

using the superstructure as a sail to reduce fuel consumption. Bot P. et al. (2012) optimized sail fiber-reinforced composites using nonlinear finite element modeling. Yeongmin Jo et al. (2013) analyzed NACA 0012 with a flap system for high lift. Robert et al. (2013) examined arc sail models, analyzing thrust, lift, and optimal sail angles.

III. OBJECTIVE

The expansion of international ocean-borne trade drives efforts to reduce marine fuel costs through conservation or alternative energy sources. Wind energy, widely available in international waters, is a promising solution. While research on wind sail propulsion exists, limited focus has been given to symmetric airfoil wind sail profiles and geometry modifications for enhanced lift. This study aims to analyze different sail geometries using CFD, select optimal sail models based on lift and drag coefficients, validate simulation results through wind tunnel experiments, and determine sail angles that maximize driving force at varying wind angles, improving efficiency in maritime transportation.

IV. METHODOLOGY

4.1 Domain and Mesh study

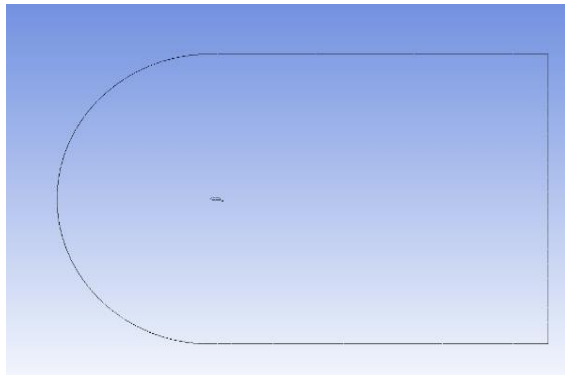


Fig 1 (C-section domain)

This is the domain which is used for the simulations. This is a C-section domain. The radius of the C-section should be at least 10 times the chord length. The length of the rectangular section should be a minimum of 15 times the chord length. Here we put the radius of the curve as 200m and the length of rectangular section as 440m.

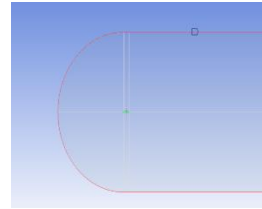


Fig 2 (Inlet of the flow)

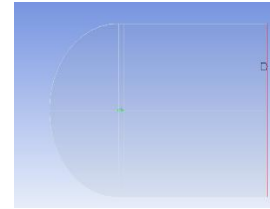


Fig 3 (outlet of the flow)

Now for Phase 1 of this work we had used a structured mesh. In the mesh of NACA 0018 it has 226000 nodes and 225000 elements. With a Y^+ value which is closer to one.

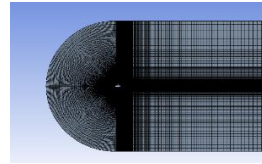


Fig 4 (structured mesh)

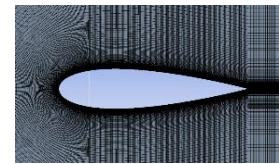


Fig 5 (Close-up image)

During the commencement of the work, there was difficulty in getting structured mesh for the modified geometries. Therefore, we used unstructured mesh which is a tri-mesh. When the same NACA0018 airfoil was meshed we got 33934 nodes and 66864 elements in unstructured meshing. We got the same and accurate results with both mesh types. Therefore, we used unstructured tri-mesh instead of structured mesh for the further simulations because of the easiness of drawing the geometry, meshing and the load given the processor is less compared to the structured mesh.

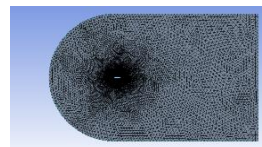


Fig 6 (tri-mesh)

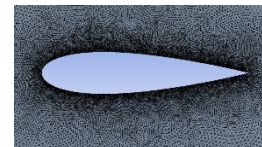


Fig 7 (Close-up image)

4.2 Software and Equipment's Used

4.2.1 ANSYS Fluent Student Version

ANSYS Fluent is a powerful CFD software used for simulating fluid flow and heat transfer. The student version provides essential features for educational purposes, including turbulence models, multiphase flow, and fluid-structure interaction analysis. Despite limitations on problem size and commercial use, it allows students to gain hands-on experience in real-world engineering simulations, enhancing their understanding of fluid dynamics and computational tools.

4.2.2 3D Printer

We used the Fractal Works Julia Advanced 3D Printer (435mm x 445mm x 385mm) to create medium-sized prototypes. Using materials like PLA and ABS, it supports applications in mechanical design, architecture, and biomedical fields. Access to a 3D printer helps students bring design concepts to life, refine prototypes, and develop skills in additive manufacturing, fostering innovation and practical learning.

4.2.3 Wind Tunnel

The wind tunnel at Viswajyothi College of Engineering and Technology (600mm x 600mm x 2000mm) provides a controlled environment for aerodynamic studies. It allows students to analyze airflow characteristics, lift and drag forces, and boundary layer behavior. By adjusting airflow rate and angle of attack, it supports prototype testing, computer model validation, and aerodynamic research, enhancing learning for aeronautical and mechanical engineering students.

4.3 Analysis and Validation of Airfoils

This study evaluates four NACA airfoils (0012, 0015, 0018, 0020) on a 2D sail model (20m width) using ANSYS FLUENT. Simulations consider eleven attack angles (0–20° in 2° steps) with a wind speed of 7.716m/s (15 knots). A wind tunnel test for NACA 0012 validates software results. The process includes geometric modeling, mesh generation, setting boundary conditions, solving Navier-Stokes equations, and calculating aerodynamic coefficients.

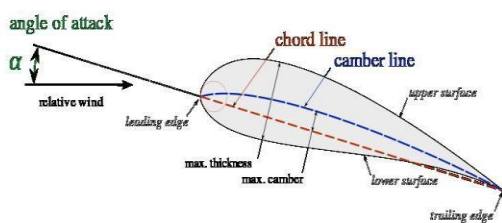


Fig 9 (Angle of attack)

Post-processing involves analysing the simulation results to extract coefficient of lift (Cl) and coefficient of drag (Cd) data for each aerofoil at various angles of attack. The optimal sail design is determined by maximizing Cl and minimizing Cd for all wind angles. This selection criterion ensures that the chosen wing provides excellent lift and minimal drag, which is crucial for efficient sailing.

By systematically comparing the aerodynamic characteristics of different wind conditions, this analysis aims to provide insight into the design of the most suitable sail to achieve optimal performance in terms of lift and drag characteristics.

Sl.No	Parameter	Setting
1	Solver	2D Segregated, steady, Implicit
2	Velocity formulation	Magnitude and Direction
3	Viscous model	Realizable k- ω
4	Pressure-velocity coupling	coupled
5	Momentum discretization	Second order upwind scheme
6	Turbulent kinetic energy and energy rate discretization	Second order upwind scheme

Table 1: Solver parameters used for simulations

A total of 44 simulations were done and favourable values for Cl and Cd were obtained.

4.3.1 Experimental Investigation on NACA 0012 for Solver Validation

A wind tunnel experiment was conducted to validate CFD results for the NACA 0012 airfoil by measuring lift and drag forces. The NACA 0018 profile (100mm chord) was analyzed at angles of attack from 0° to 14° in 2° steps. Results showed that increasing the Reynolds number decreases lift and drag forces for a fixed chord length, while larger chords increase CL and CD. The study compared experimental and CFD results, conducted in a subsonic wind tunnel (600mm x 600mm x 2000mm) at Viswajyothi College of Engineering and Technology, Kerala.

Forward thrust and lateral thrust calculated from the coefficient of lift (Cl) and coefficient of drag (Cd) from the equations:

- Coefficient of Lateral Thrust = $Cl \cdot \sin(\alpha) - Cd \cdot \cos(\alpha)$
- Coefficient of Forward Thrust = $Cl \cdot \cos(\alpha) + Cd \cdot \sin(\alpha)$

4.4 MODIFICATION OF GEOMETRY

This stage focuses on optimizing the wind sail geometry by changing the symmetrical aerodynamic section at certain curvature points and adjusting the tip angle. The goal of this optimization process is to improve the efficiency of the sailboat in generating forward thrust while minimizing lateral thrust.

The geometry of the sail is changed by bending the symmetrical aerodynamic section at six different points: 10%, 20%, 30%, 40%, 50% and 60% along the chord length. In addition, the tip angle is changed up to 50 degrees in 10-degree steps.

Angle of Tip / % of Chord Length	10 Deg	20 Deg	30 Deg	40 Deg	50 Deg
10%					
20%					
30%					
40%					
50%					
60%					

Fig 13 (Modification of geometry)

Simulations are performed using ANSYS FLUENT at seven different wind angles from 0 to 20 degrees in 2degree increments. During simulation runs, modified sail geometries are analysed based on their ability to generate maximum forward and minimum lateral thrust.

Thrust components are calculated using the following equations:

- Coeff. of Forward thrust = $L \cdot \sin(\alpha) - D \cdot \cos(\alpha)$

- Coeff. of Lateral thrust = $L \cdot \cos(\alpha) + D \cdot \sin(\alpha)$

Where:

- α represents the angle of attack,

- L represents the lift coefficient.

- D represents the drag coefficient.

4.5 FABRICATION AND SMOKE TEST

4.5.1 Fabrication of the selected geometry:

A prototype model of the selected 30° bended NACA 0018 airfoil with a 40% chord length modification is fabricated using the 3D printer shown in Fig 14. This model of the airfoil is used to conduct the smoke test. The printed model has an extruded length of 150mm with airfoil cross-sectional horizontal length of 91.4mm and it has a hole of diameter 11mm for the support of it into the smoke test section.

After applying the parameters and settings we will get our finished product as shown below:



Fig 14 (Image of model being printed)

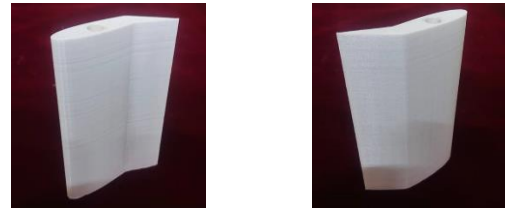


Fig 15 (Finished image of model)

4.5.2 Experimental Smoke Testing Using Wind Tunnel:

Using smoke particles, the airflow patterns surrounding an airfoil are visualized during an experimental smoke test on a wind tunnel equipment. Smoke is injected into the airflow while the airfoil is positioned inside the wind tunnel for this test. The smoke particles stick to the air currents created by the wind tunnel, exposing the flow patterns surrounding the airfoil's surface. Through the tracking of smoke particle movement and dispersion, we can learn more about aerodynamic phenomena such flow separation, boundary layer activity, and vortex generation. The data obtained from this experimental technique is highly valuable for the analysis and optimization of airfoil designs, hence improving their performance and efficiency in a variety of applications such as hydrofoils, wind turbines, and aircraft wings.

V. RESULTS AND DISCUSSION

5.1 Validation of NACA0012 with CFD results

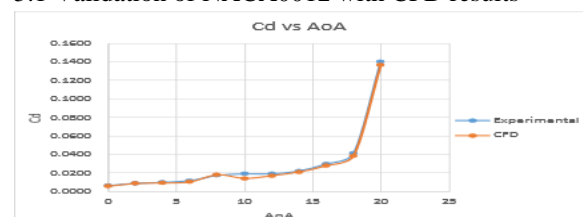


Fig 17 (Cd v/s AoA graph of experimental and CFD analysis)

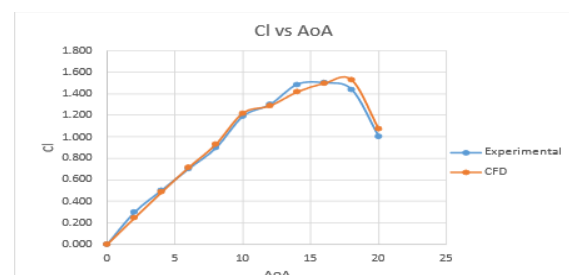


Fig 18 (Cl v/s AoA graph of experimental and CFD analysis)

The graphs above show the experimental values of NACA 0012 and CFD values of NACA 0012 side by side. Based on these graphs we can ensure that the solver parameters and settings we taken to conduct the simulations are correct and we can take it also for the analysis of the other airfoils also.

5.2 Co-efficient of lift (Cl) & Co-efficient of drag (Cd) of the four airfoils:

NACA 0012			NACA 0015		
AoA	Cl	Cd	AoA	Cl	Cd
0	0.0000	0.00557	0	0.0000	0.00896
2	0.2440	0.00850	2	0.2400	0.00916
4	0.4840	0.00910	4	0.4772	0.00976
6	0.7140	0.01020	6	0.7040	0.01070
8	0.9290	0.01800	8	0.9157	0.01230
10	1.1219	0.01400	10	1.1050	0.01430
12	1.2870	0.01700	12	1.2680	0.01716
14	1.4160	0.02100	14	1.3950	0.02100
16	1.4960	0.02780	16	1.4769	0.02667
18	1.5275	0.03849	18	1.5135	0.03570
20	1.0700	0.13650	20	1.4170	0.06100

NACA 0018			NACA 0020		
AoA	Cl	Cd	AoA	Cl	Cd
0	0.0000	0.0096	0	0.0001	0.0090
2	0.2370	0.0098	2	0.2250	0.0098
4	0.4618	0.0104	4	0.4490	0.0103
6	0.6828	0.0114	6	0.6663	0.0113
8	0.8889	0.0128	8	0.8695	0.0127
10	1.0738	0.0149	10	1.0519	0.0147
12	1.2309	0.0177	12	1.2060	0.0170
14	1.3520	0.0215	14	1.3260	0.0210
16	1.4319	0.0274	16	1.4080	0.0272
18	1.4617	0.0370	18	1.4420	0.0365
20	1.3512	0.0630	20	1.3430	0.0605

Table 2 : All Cl & Cd values

5.3 Comparison of Co-eff of LT & FT of the four airfoils:

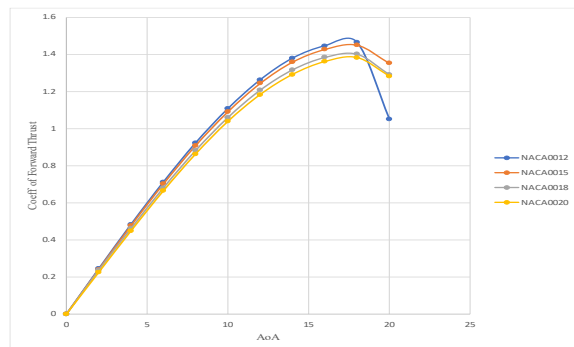


Fig 19 (Coefficient of Forward Thrust v/s AoA)

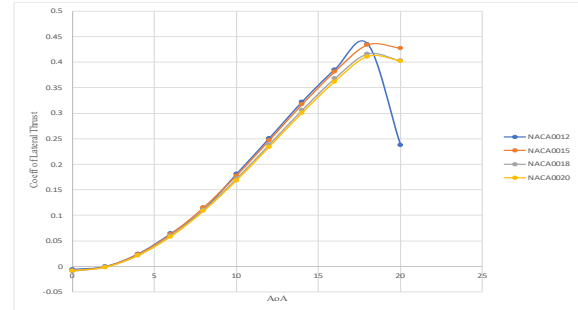


Fig 20 (Coefficient of Lateral Thrust v/s AoA)

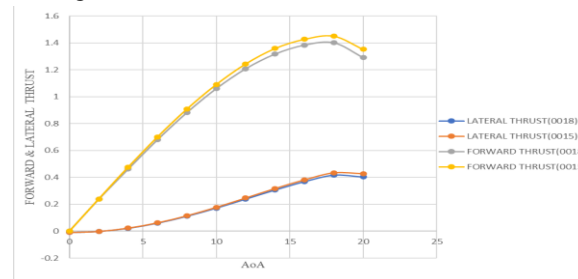


Fig 21 (LT&FT of 0018 & 0015 v/s AoA)

Based on the analysis of the obtained graph, it has been determined that the airfoil NACA 0012 exhibit irregular behaviour. The decision to eliminate NACA 0020 was influenced by its low forward thrust value, rendering it unsuitable for the intended application. Conversely, the remaining airfoils, namely NACA 0015 and NACA 0018, have demonstrated more favourable performance attributes and have thus advanced to the next phase of the selection process.

It is clear from examining the graph that NACA 0015 has greater forward and lateral thrust coefficients than NACA 0018. Still, practical factors must be taken into account while determining their viability for ship propulsion. In practical applications, lateral thrust can cause a ship to veer off course, which may need using more fuel to get back on course. Consequently, choosing an airfoil with a higher coefficient of lateral thrust may result in using more fuel. In light of this, NACA 0018 is selected for further assessment. Despite having marginally lower thrust coefficients than NACA 0015, the two airfoils differences in forward thrust coefficients are so small that they are unlikely to cause significant issues in practical applications. From the 4 airfoils NACA 0018 has been selected for further assessment. Comparison of the wind tunnel experiment of NACA 0012 with its CFD values proved the

credibility of the solver parameters and settings we took

5.4 Results from the Modification of Geometry of NACA0018

The co-efficients of LT & FT at 0° AoA

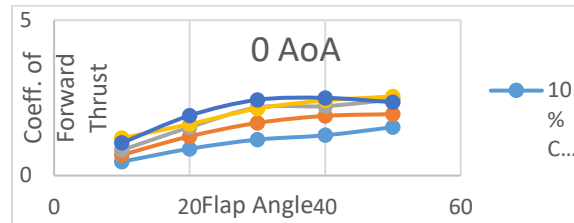


Fig 22 (Co-efficient of forward thrust v/s 0° AoA)

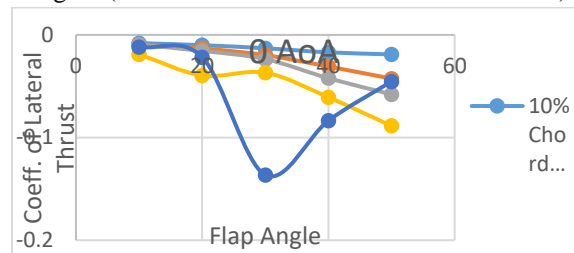


Fig 23 (Co-efficient of lateral thrust v/s 0° AoA)

The co-efficients of LT & FT at 2° AoA

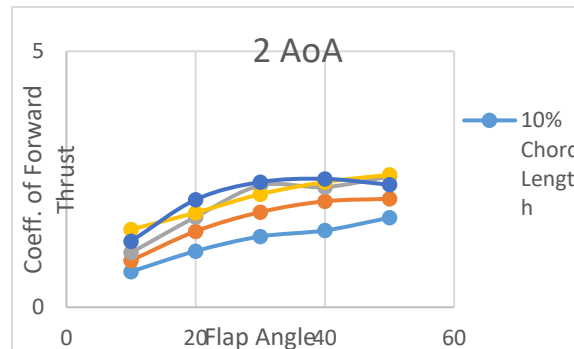


Fig 24 (Co-efficient of forward thrust v/s 2° AoA)

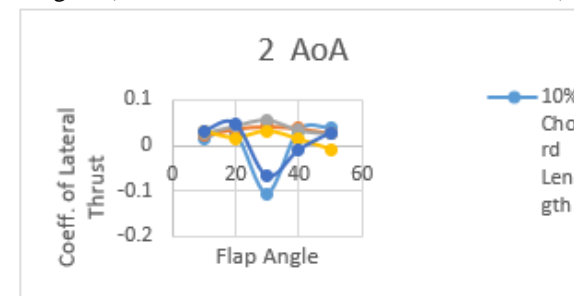


Fig 25 (Co-efficient of lateral thrust v/s 2° AoA)

The co-efficients of LT & FT at 4° AoA

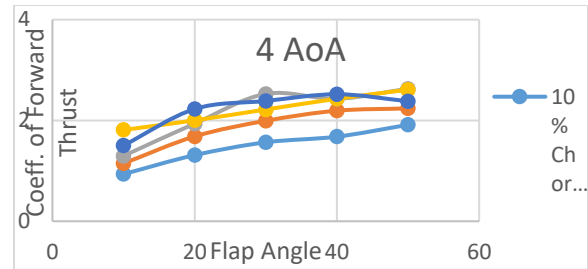


Fig 26 (Co-efficient of forward thrust v/s 4° AoA)

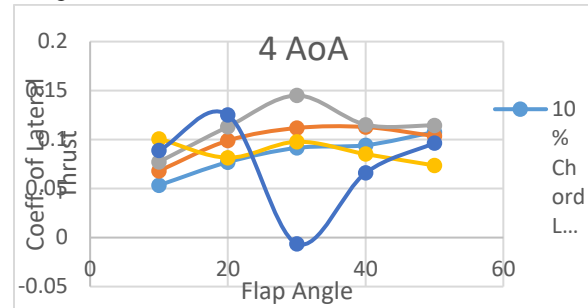


Fig 27 (Co-efficient of lateral thrust v/s 4° AoA)

The co-efficients of LT & FT at 6° AoA

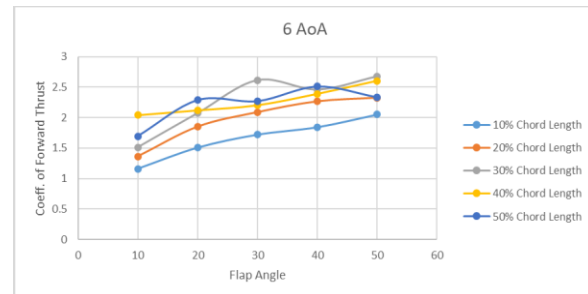


Fig 28 (Co-efficient of forward thrust v/s 6° AoA)

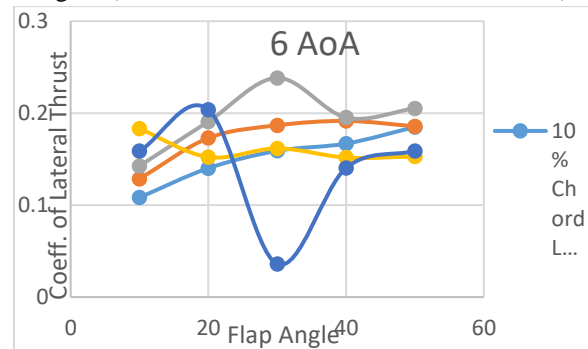


Fig 29 (Co-efficient of lateral thrust v/s 6° AoA)

The co-efficients of LT & FT at 8° AoA

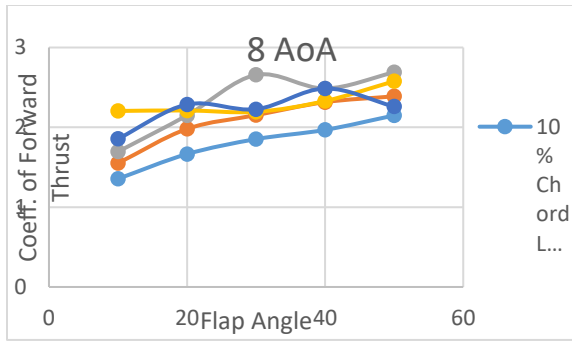


Fig 30 (Co-efficient of forward thrust v/s 8° AoA)

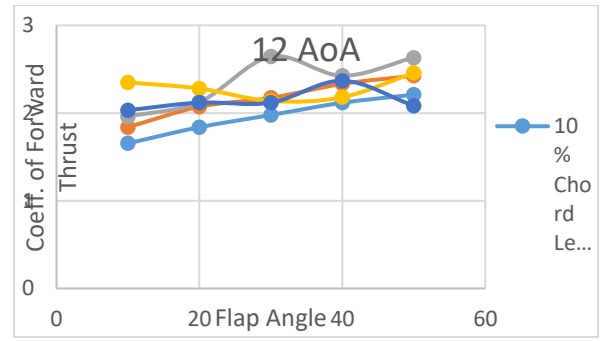


Fig 34 (Co-efficient of forward thrust v/s 12° AoA)

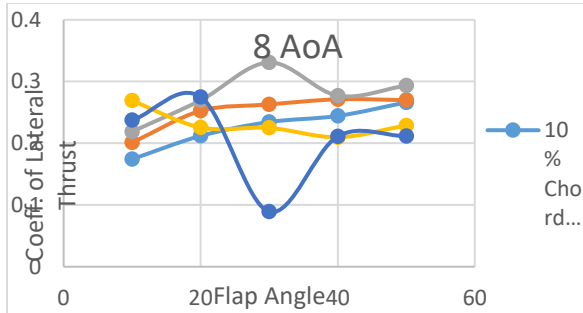


Fig 31 (Co-efficient of lateral thrust v/s 8° AoA)

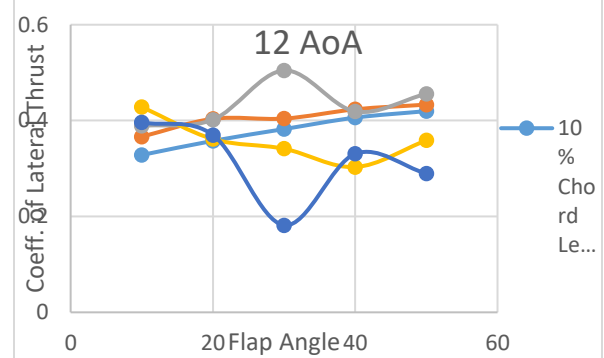


Fig 35 (Co-efficient of lateral thrust v/s 12° AoA)

The co-efficients of LT & FT at 10° AoA

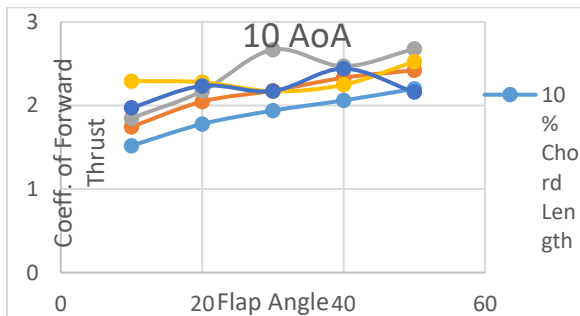


Fig 32 (Co-efficient of forward thrust v/s 10° AoA)

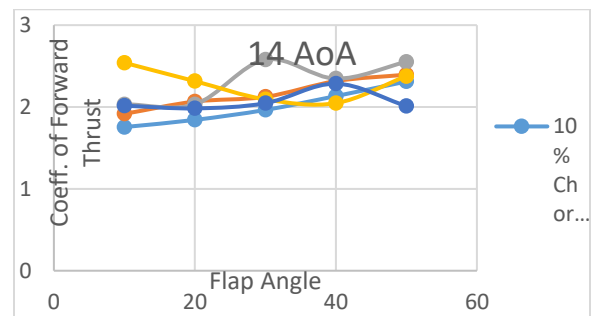


Fig 36 (Co-efficient of forward thrust v/s 14° AoA)

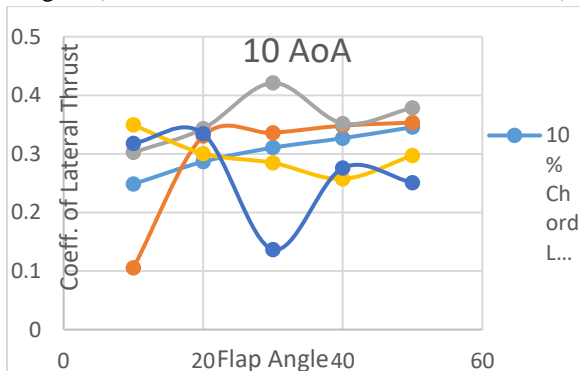


Fig 33 (Co-efficient of lateral thrust v/s 10° AoA)

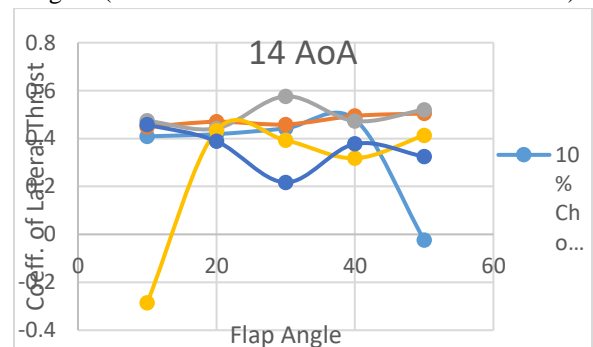


Fig 37 (Co-efficient of lateral thrust v/s 14° AoA)

The co-efficients of LT & FT at 12° AoA

The co-efficients of LT & FT at 16° AoA

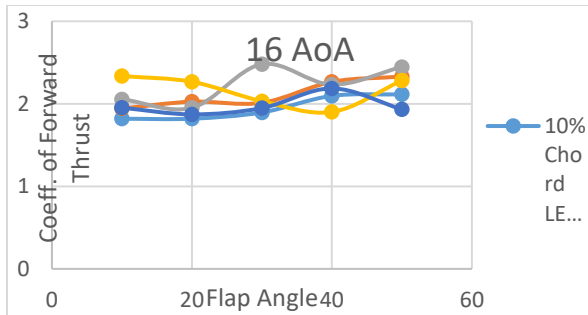


Fig 38 (Co-efficient of forward thrust v/s 16° AoA)

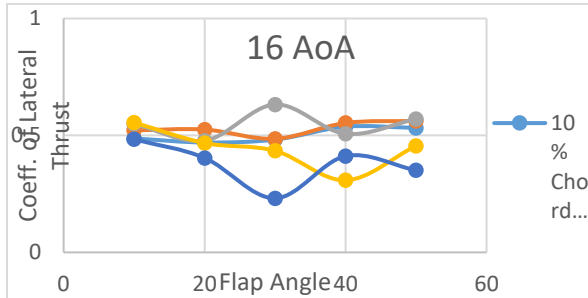


Fig 39 (Co-efficient of lateral thrust v/s 16° AoA)

The co-efficients of LT & FT at 18° AoA

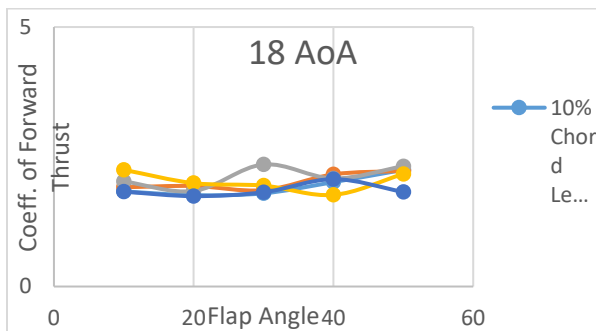


Fig 40 (Co-efficient of forward thrust v/s 18° AoA)

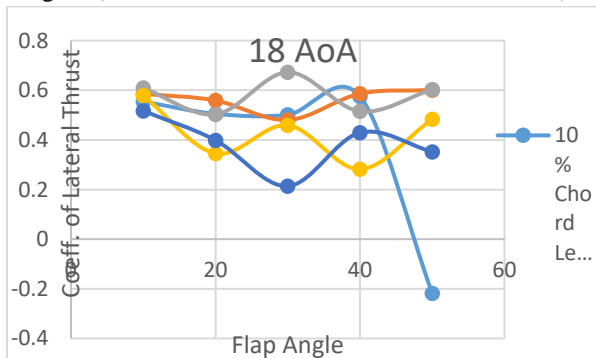


Fig 41 (Co-efficient of lateral thrust v/s 18° AoA)

The co-efficients of LT & FT at 20° AoA

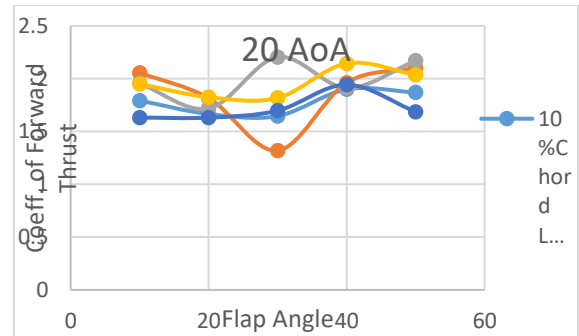


Fig 42 (Co-efficient of forward thrust v/s 20° AoA)

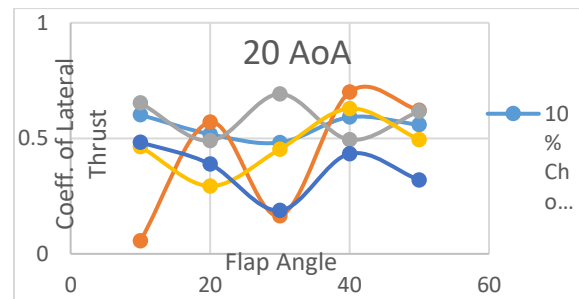


Fig 43 (Co-efficient of lateral thrust v/s 20° AoA)

By analyzing the performance graphs of each modified sail geometry under various wind angles and visibility, we can see that the airfoils with 30% and 40% chord length bended show more promising and progressive steady values in forward thrust than the other modified geometries. Also, these values are maximum at the 30° angle of bending of the airfoils. But when it comes to lateral thrust, the 40% chord length-bended airfoil has more satisfactory values compared to the 30% chord length-bended airfoil. From these inferences, we take the 30° bended at 40% chord length bended airfoil as the selection criterion so that this selected sail geometry provides excellent thrust and stability, which is crucial for efficient wind-powered navigation. The analysis indicates that the 30° bended NACA 0018 airfoil with a 40% chord length modification emerges as the optimal sail geometry, offering superior forward thrust and satisfactory lateral thrust, thereby ensuring efficient wind-powered navigation with enhanced thrust and stability.

5.5 Smoke Test

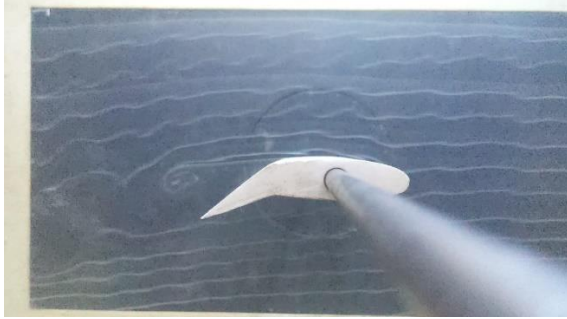


Fig 44 (Smoke test image of the airfoil)

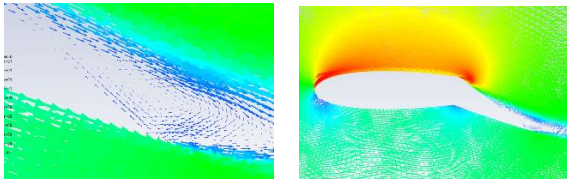


Fig 45 (CFD images of velocity streamlines around the airfoil)

Based on the results of smoke test done in the wind tunnel, we can observe that the smoke test image of the airfoil at zero-degree angle of attack and comparing it with that of the CFD simulations of the airfoil at same conditions shows similar flow and characteristics. Thrust given by the airfoil will also be similar because of similar streamlines around the airfoil in both the cases. There is a vortex formed around the tip of the airfoil both in experimentation and CFD analysis. We can observe high pressure and low pressure zones below and above airfoil which gives the airfoil its lift. From these inferences the CFD results, and experimental results are validated.

VI. CONCLUSION

From the analysis of 4 standard airfoils (NACA 0012, NACA 0015, NACA 0018, NACA 0020) using ANSYS FLUENT, the airfoil profile of NACA 0012 was analyzed for the validation of the solver settings. The selected NACA profile from the above four airfoils was analyzed using CFD techniques and modification of its geometry to study the performance of the profile. The selected NACA profile i.e. NACA0018 was modified with the addition of a flap at different positions of the chord length (10%, 20%, 30%, 40%, 50%). Step-by-step modification of the selected symmetrical standard airfoil section was carried out. These modified sections were analyzed for the maximum

driving force from the sail. The chosen NACA 0018 model is modified with a flap at 40% chord. The optimum flap is found to be 30 degrees. The angle is chosen as 30 deg as it produces sufficient forward thrust with manageable lateral thrust.

REFERENCES

- [1] K. Prasanth, M.N Senthil Prakash and K. Sivaprasad. 2021. Optimization of Wind Sail using Computational Fluid Dynamics Simulation. *Int. J. Vehicle Structures & Systems*, 13(4),1-5.
- [2] Yihuai Hu and Jianhai He (2015), "Sail Structure Design and Stability Calculation for Sail-assisted Ships". *Marine Engineering Frontiers (MEF)* Vol 3, 2015.
- [3] Yong Ma (2018) "New insights into airfoil sail selection for sail-assisted vessel with computational fluid dynamics simulation" *Advances in Mechanical Engineering*, Volume 10, Issue 4, April 2018.
- [4] Viola IM (2009) "Downwind sail aerodynamics: A CFD investigation with high grid resolution", *Ocean Engineering*, Vol 36, 974- 984. Auckland, New Zealand.
- [5] Flay R, Richard GJ, Viola IM (2011) "Sail pressures from full-scale", wind-tunnel and numerical investigations, *Ocean Engineering*, Vol 38, 1733–1743.
- [6] Siulisetoyo A, Nasurudeen A (2010) "Wind sail analysis using CFD simulation", *Proceedings of MARTEC 2010*.
- [7] Collie SJ, Jackson P, Gerritsen M (2002) Validation of CFD Methods for Downwind Sail Design. In proceedings of the High-Performance Yacht Design Conference, Auckland, New Zealand.
- [8] Francisco Perez A, Patricia A, Luis P, Rojas B and Alberto Torres B (2012) *Procedia - Social and Behavioural Sciences* 48 "EU- Cargo Xpress: Wind Propulsion Concept" pp 1314 – 1323, Victoria, 20844, Madrid.
- [9] Bot P, Viola IM and Riotte M (2012) "Upwind sail aerodynamics: A RANS numerical investigation validated with wind tunnel pressure measurement" *International Journal of Heat and Fluid Flow*, Vol 38, 90-101.